Supporting information for

Dual-Mode Waveguiding of Raman and Luminescence Signals in a Crystalline Organic Microplate

Seong-Gi Jo [a†], *Dong Hyuk Park* [b,c†], *Bong-Gi Kim* [b†], *Sungbaek Seo* [b], *Suk Joong Lee* [d], *Jeongyong Kim* [e*], *Jinsang Kim* [b*], *and Jinsoo Joo* [a*]

[a]Department of Physics, Korea University, Seoul 136-713, Republic of Korea

[b]Materials Science and Engineering, Macromolecular Science and Engineering, University of Michigan, Ann Arbor, Michigan 48109, USA

[c]Division of Nano-systems Engineering, Department of Advanced Fiber Engineering, Inha University, Incheon 402-751, Republic of Korea

[d]Department of Chemistry, Korea University, Seoul 136-713, Republic of Korea

[e]Center for Integrated Nanostructure Physics (CINAP), Institute of Basic Science (IBS); Department of Energy Science, Sungkyunkwan University, Suwon 440-746, Republic of Korea

† All authors contributed equally to this work.

*Corresponding authors. E-mail: jjoo@korea.ac.kr (J. Joo); Fax: +82-2-927-3292; Tel: +82-2-3290-3103
E-mail: jinsang@umich.edu (Jinsang Kim)
E-mail: j.kim@skku.edu (Jeongyong Kim)

1. Single crystal X-ray crystallography

The following X-ray diffraction data for 1,4-bis(3,5-bis(trifluoromethyl) cyanostyryl)-2,5-dibromobenzene (CN-TSDB) crystals were collected using a Bruker SMART APEX diffractometer equipped with a monochromator for a Mo Kα (λ = 0.71073 Å) incident beam. Table S1 lists the crystal data and structural refinement of the CN-TSDB microplates.

Crystal data for CN-TSDB: C_{28} H_{10} Br_2 F_{12} N_2, MW = 762.20, monoclinic (space group $P2_1/c$), a = 20.1093(5) Å, b = 4.67830(10) Å, c = 14.0181(4) Å, β = 95.8770(10)°, V = 1311.85(6) $Å^3$, Z = 2. A total of 15746 reflections were measured; of these, the 2531 that were unique (R_{int} = 0.0276) and were used in all calculations. The final R value was 0.0200 (Rw = 0.0513) for the reflections having intensities greater than 2σ; GOF (F^2) = 1.068.

Table S1. Crystal data and structure refinement of CN-TSDB microplates.

Crystal	CN-TSDB
Empirical formula	$C_{28}\ H_{10}\ Br_2\ F_{12}\ N_2$
Formula weight	762.20
Temperature (K)	100(2)
Wavelength (Å)	0.71073
Space group	$P2_1/c$
a(Å)	20.1093(5)
b(Å)	4.67830(10)
c(Å)	14.0181(4)
α(°)	90.00
β(°)	95.8770(10)
γ(°)	90.00
Volume($Å^3$)	1311.85(6)
Z	2
Density (calc.) (Mg/m^3)	1.930
Absorption coeff. (mm^{-1})	3.199
Crystal size (mm^3)	0.20 × 0.20 × 0.10
Reflections collected	15746
Independent reflections [R(int)]	2531 [R(int) = 0.0276]
Data/restraints/parameters	2531 / 0 / 199
Goodness-of-fit on F^2	1.068
Final R indices [I>2σ(I)]	R_1 = 0.0200, wR_2 = 0.0513
R indices (all data)	R_1 = 0.0233, wR_2 = 0.0524
Largest diff. peak and hole ($e.Å^{-3}$)	0.365 and -0.295

2. LCM PL mapping image and spectra

Laser confocal microscope (LCM) photoluminescence (PL) mapping experiments were performed to investigate the nanoscale luminescence characteristics of the CN-TSDB microplates. Figures S1a and S1b show the LCM PL mapping image and spectra of the CN-TSDB microplates, respectively. The luminescence brightness at the edges of the sample was relatively higher than that inside the sample interior, which can be explained by the scattering effect. LCM PL at the corners (points A and C in Figure S1a) of the microplates was much brighter. The results of this mapping were confirmed by the LCM PL spectra shown in Figure S1b.

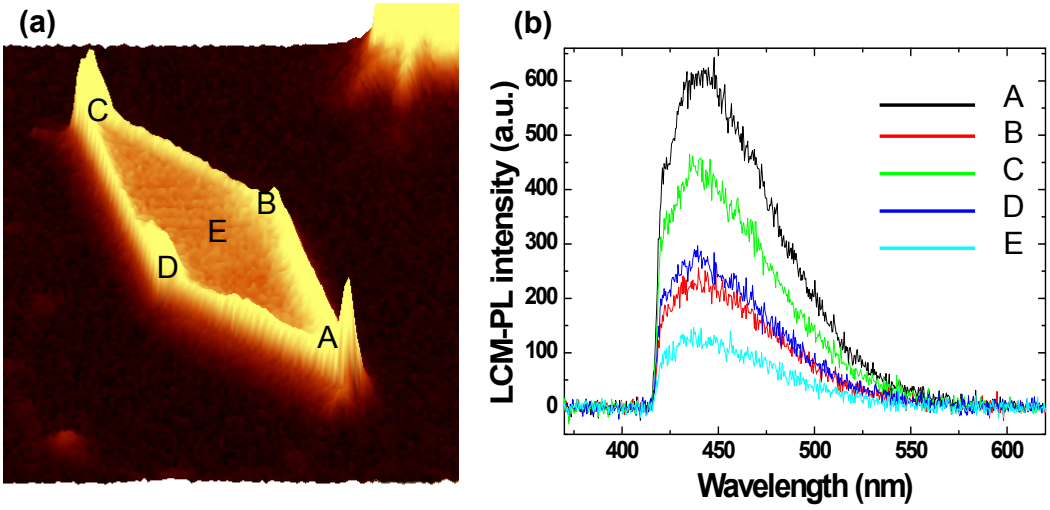

Figure S1. (a) LCM PL mapping image of a CN-TSDB microplate. (b) LCM PL spectra at the corresponding points (A, B, C, D, and E) of the CN-TSDB microplate.

3. Raman waveguiding characteristics

The Raman waveguiding characteristics of the CN-TSDB microplates in the main text (Figure 4) were investigated along various scanning directions. Table 1 lists characteristic Raman modes of the microplate (λ_{ex} = 633 nm). Figures S2a, S2b, and S2c show the waveguide-propagated Raman spectra, i.e., output Raman signals of the C–Br (667 cm^{-1}), –CF_3 (1216 cm^{-1}), and –C=C– aromatic (1594 cm^{-1}) stretching modes, respectively, along the [*A*] direction with various propagation distances. Figures S2d, S2e, and S2f also show the waveguide-propagated Raman spectra of the C–Br (667 cm^{-1}), –CF_3 (1216 cm^{-1}), and –C=C– aromatic (1594 cm^{-1}) modes, respectively, along the [*C*] direction with various propagation distances. The LCM Raman intensity decreased as propagation distance increased. The Raman waveguiding characteristics of the CN-TSDB microplates along the [*A*] and [*C*] directions were similar to those along the [*B*] direction.

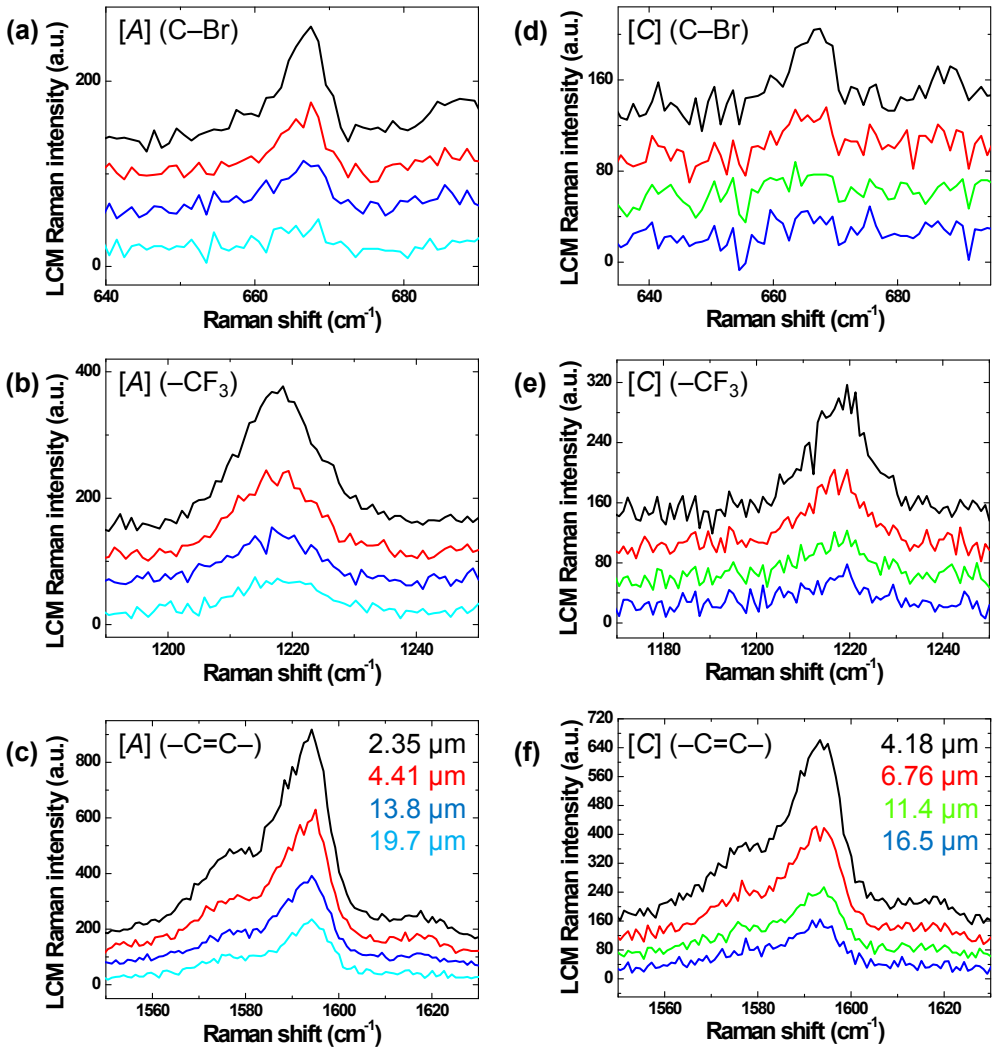

Figure S2. Waveguide-propagated LCM Raman spectra, i.e., output Raman signals, from a CN-TSDB microplate for the (a) C–Br, (b) $–CF_3$, and (c) –C=C– aromatic modes along the [*A*] direction and (d) C–Br, (e) $–CF_3$, and (f) –C=C– aromatic modes along the [*C*] direction.

To confirm the Raman waveguiding characteristics, we repeated our experiments using samples from another batch of CN-TSDB microplates. Figures S3, S4, and S5 show the Raman waveguide characteristics of the CN-TSDB microplates from another batch. Figures S3 and S4 show the characteristic C–Br, $–CF_3$, and –C=C– aromatic Raman modes that were propagated through the microplate. We also observed that the decay constant increased with increasing Raman shift, as shown in Figure S5, which is qualitatively consistent with the results in Figure 5.

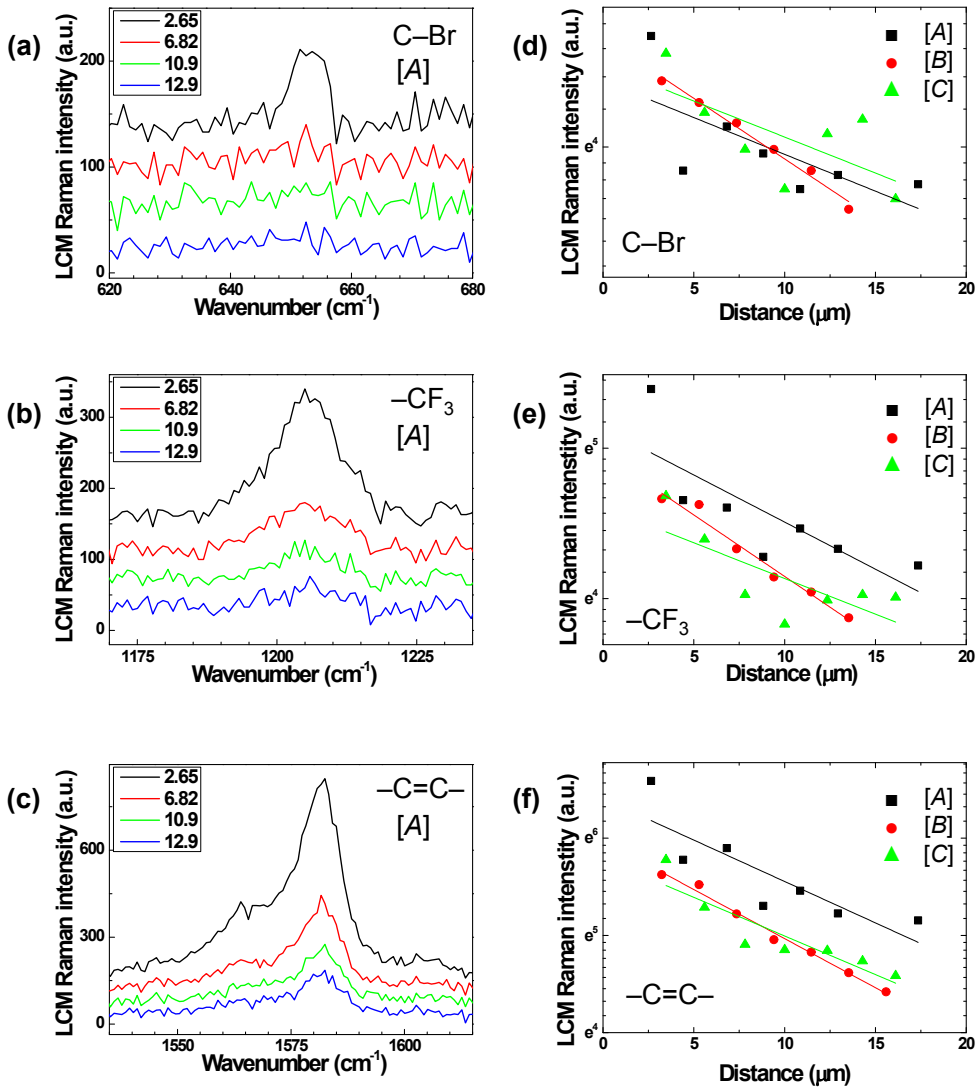

Figure S3. Waveguide-propagated LCM Raman spectra of the (a) C–Br, (b) $–CF_3$, and (c) –C=C– aromatic stretching modes along the [*A*] direction with varying propagation distances (inset). LCM Raman intensity of the (d) C–Br (652 cm^{-1}), (e) $–CF_3$ (1205 cm^{-1}), and (f) –C=C– aromatic (1582 cm^{-1}) stretching modes versus the propagation distance along the [*A*], [*B*], and [*C*] directions

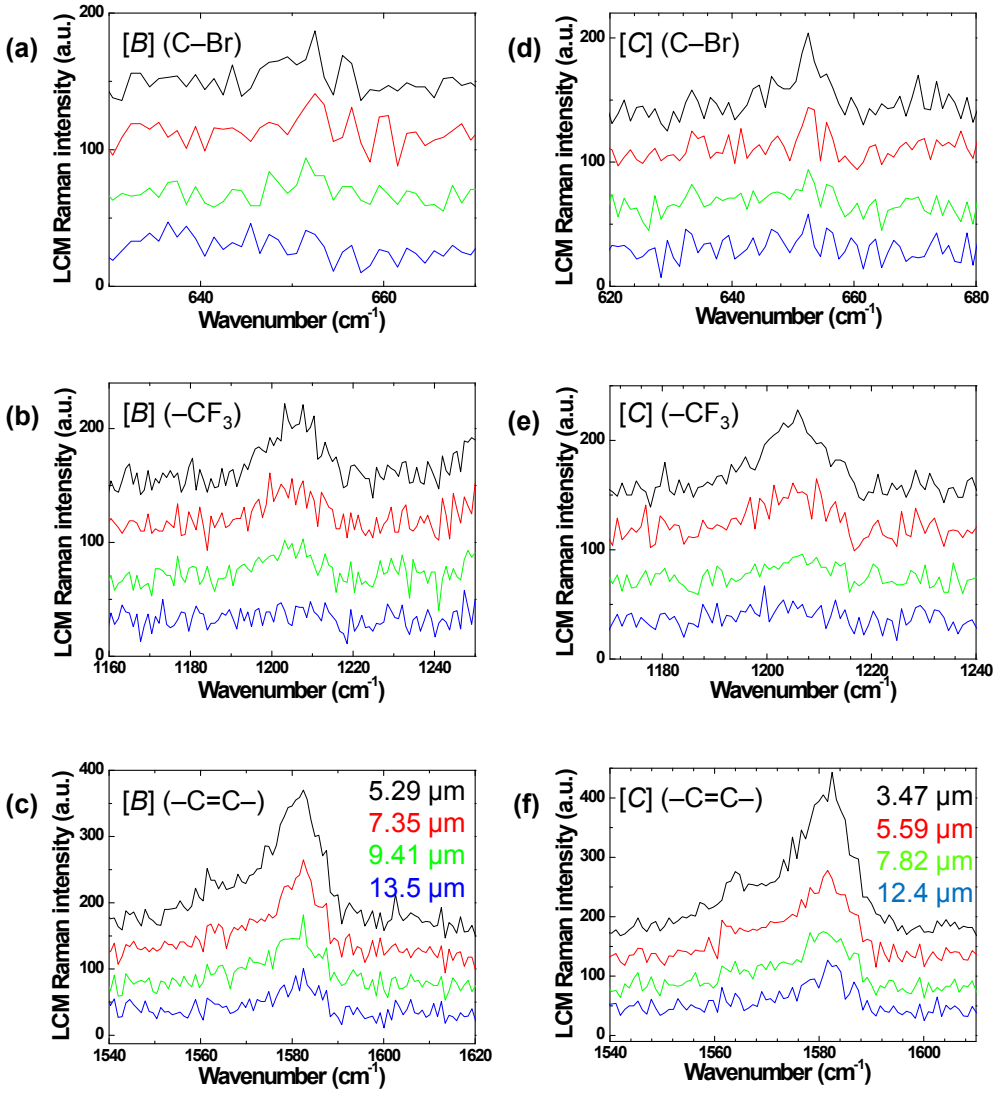

Figure S4. (a), (b), and (c) Waveguide-propagated LCM Raman spectra, i.e., output Raman signals, from the CN-TSDB microplate along the [*B*] direction. (d), (e), and (f) Waveguide-propagated LCM Raman spectra of CN-TSDB microplate along the [*C*] direction.

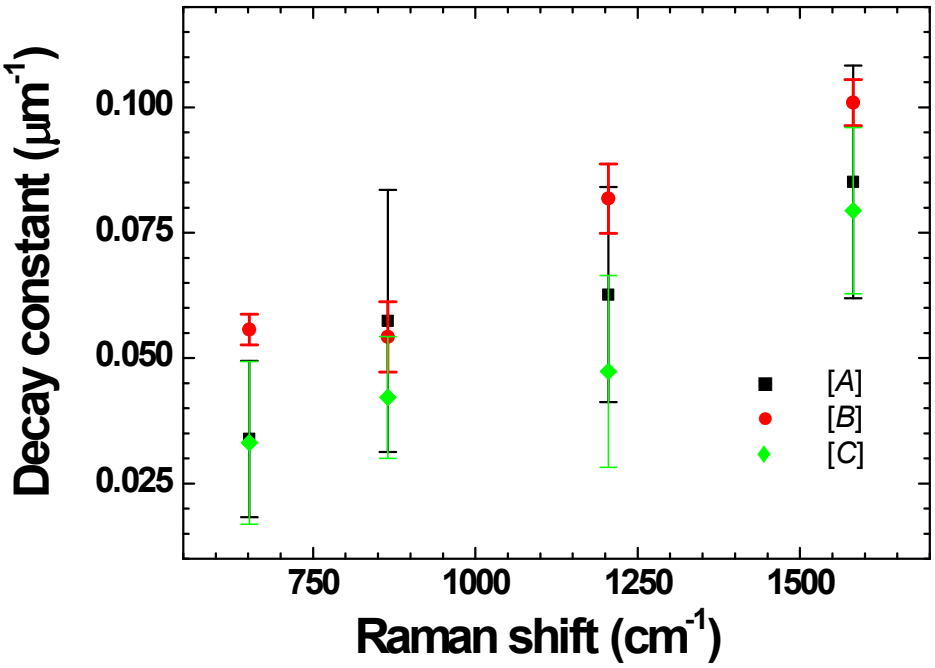

Figure S5. Plot of the decay constant (μm^{-1}) of the Raman intensity versus Raman shift (cm^{-1}) along the [*A*], [*B*], and [*C*] directions.

4. AFM images

We performed atomic force microscope (AFM; NanoFocus Ltd., Albatross) experiments to investigate the surface morphology and dimensions of the CN-TSDB microplates. Figures S6a-c show the AFM images and line profiles for a different batch of CN-TSDB microplates. The first row in Figure S6 shows top view images, the second row shows three-dimensional (3D) view images, and the third and fourth rows show cross-sectional profiles along the (01) (blue line) and (02) (red line) directions, respectively, for different CN-TSDB microplates. From the AFM images, it was determined that the CN-TSDB microplates have a diamond shape with dimensions and thicknesses between 12–24 μm and 400–500 nm, respectively. The surfaces of the microplates are nearly flat. However, some of the CN-TSDB microplates exhibit a convex shape at their center, as shown in Figure S6b.

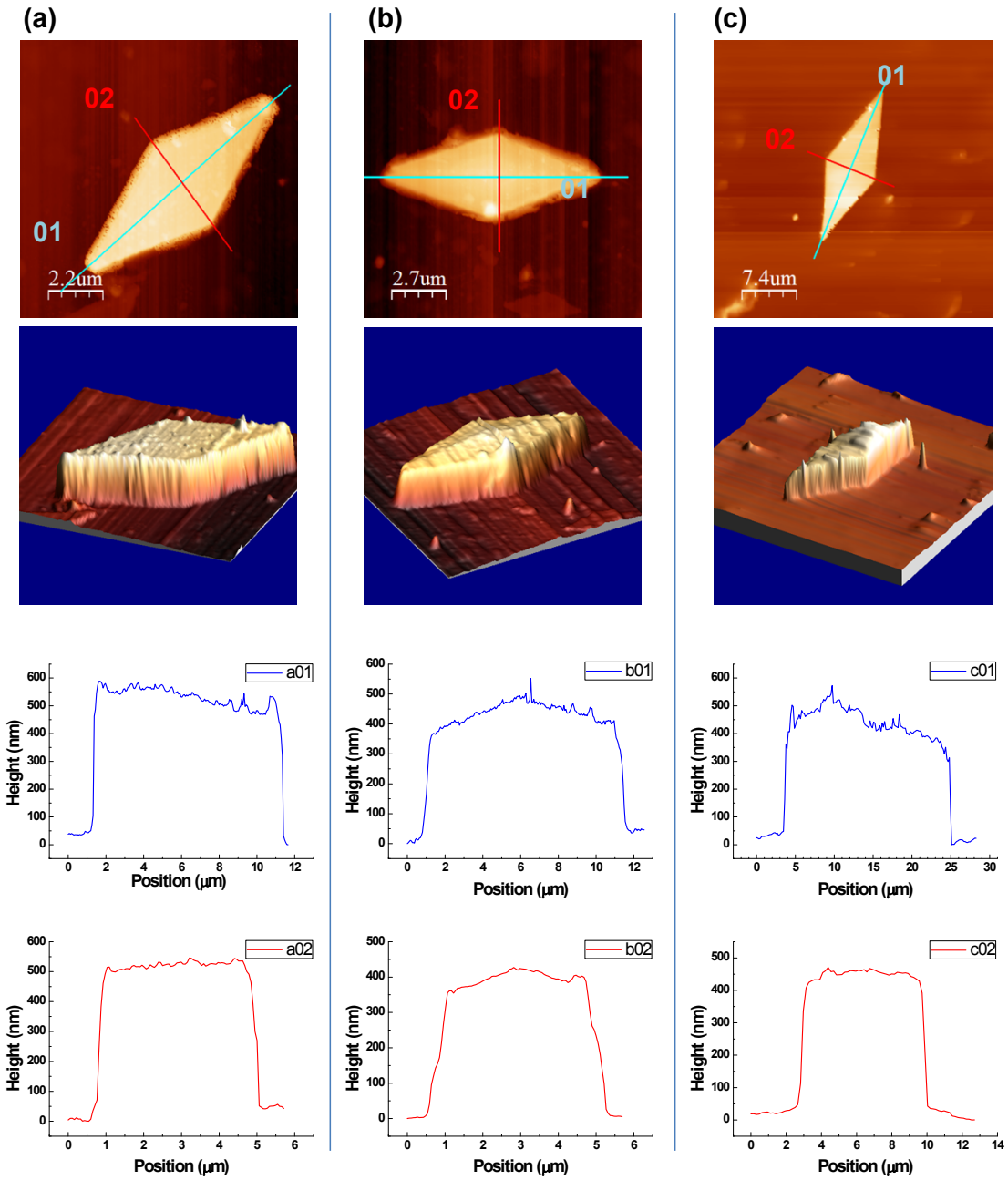

Figure S6. AFM images and their analysis of the CN-TSDB microplates. Images in the first, second, third, and fourth rows are the top view, 3D AFM view, and cross-sectional profiles along (01) (blue line) and (02) (red line) directions, respectively, for different microplates.